JOURNAL OF MAGNETIC RESONANCE IMAGING 40:804–812 (2014)

Original Research

Dielectric Pads and Low-B_1^+ Adiabatic Pulses: Complementary Techniques to Optimize Structural T_1w Whole-Brain MP2RAGE Scans at 7 Tesla

Kieran R. O'Brien, PhD,[1,2,3]* Arthur W. Magill, PhD,[3] Jean Delacoste, MS,[3] Jose P. Marques, PhD,[3,4] Tobias Kober, PhD,[2,3] Hans-Peter Fautz, PhD,[5] Francois Lazeyras, PhD,[1] and Gunnar Krueger, PhD[2,3]

Purpose: To evaluate the combination of low-B_1^+ adiabatic pulses and high permittivity ($\varepsilon_r \approx 165$) dielectric pads effectiveness to reproducibly improve the inversion efficiency for whole-brain MP2RAGE scans, at ultra-high field.

Materials and Methods: Two low-B_1^+ adiabatic pulses, HS8 and TR-FOCI, were compared with the conventional HS1 adiabatic pulse in MP2RAGE acquisitions of four subjects at 7 Tesla. The uniform MP2RAGE images were qualitatively assessed for poor inversion artifacts by trained observers. Each subject was rescanned using dielectric pads. Eight further subjects underwent two MP2RAGE scan sessions using dielectric pads and the TR-FOCI adiabatic pulse.

Results: The HS8 and TR-FOCI pulses improved inversion coverage in all subjects compared with the HS1 pulse. However, in subjects whose head lengths are large ($\geq$136 mm) relative to the coil's z-coverage, the B_1^+ field over the cerebellum was insufficient to cause inversion. Dielectric pads increase the B_1^+ field, by ~50%, over the cerebellum, which in conjunction with the TR-FOCI pulse, reproducibly improves the inversion efficiency over the whole brain for subjects with head lengths $\leq$155 mm. Minor residual inversion artifacts were present in three of eight subjects (head lengths $\geq$155 mm).

Conclusion: The complementary techniques of low-B_1^+ adiabatic RF pulses and high permittivity dielectric pads allow whole-brain structural T_1w images to be reliably acquired at ultra-high field.

Key Words: morphometry; structural imaging; ultra-high field; brain; dielectric pads
J. Magn. Reson. Imaging 2014;40:804–812.

THE LARGER STATIC (B_0), transmit (B_1^+) and receive (B_1^-) radiofrequency (RF) field inhomogeneities at ultra-high field ($\geq$7 Tesla [T]) makes the acquisition of high quality whole-brain structural scans challenging. A new sequence, Magnetization Prepared with 2 Rapid Gradient Echoes (MP2RAGE) (1,2), has recently been introduced that provides the so-called "uniform image," which has self-correcting properties for the receive bias field, T2* relaxation and proton density. As long as the adiabatic condition of the inversion pulse is met, the remaining transmit B_1^+ homogeneities will either be minimal (1) or can be corrected for with the aid of a B_1^+ map (3). Otherwise, if the adiabatic condition of the inversion pulse is not met, the artifacts remaining on the "uniform image" are not correctable. Consequently, regions of the human brain that experience a low-B_1^+ at ultra-high fields, such as the cerebellum and temporal lobes, often exhibit poor inversion resulting in degradation of image quality. Furthermore, when the acquired volumes are used for brain morphometry, these inversion artifacts severely impede the use of whole-brain segmentation. In particular, it is critical to be able to estimate the total intracranial volume (4) from the T_1w image, to normalize the volumes of substructures, to reduce inter-individual variation, and to enable longitudinal comparisons. These inversion inefficiencies lead to a major limitation in the use of MPRAGE-type structural T_1w 7T scans compared with T_1w 3T scans, in both clinical and research settings (2,5–7).

At 7T, the larger frequency sweep required by the conventional hyperbolic secant (HS1) adiabatic pulse to invert areas with large B_0 inhomogeneities, such as the sagittal sinus, increases the B_1^+ required to fulfill the adiabatic condition (8). This adiabatic threshold

[1]CIBM_IRM HUG, Department of Radiology, University of Geneva, Geneva, Switzerland.
[2]Advanced Clinical Imaging Technology, Siemens Healthcare IM S AW, Renens, Switzerland.
[3]CIBM AIT, École polytechnique fédérale de Lausanne, Lausanne, Switzerland.
[4]CIBM AIT, Department of Radiology, University of Lausanne, Lausanne, Switzerland.
[5]Siemens AG, Healthcare Sector, Erlangen, Germany.
*Address reprint requests to K.R.O., EPFL SB IPSB LIFMET, Station 6, CH- 1015 Lausanne, Switzerland. E-mail: kieran.obrien@epfl.ch
Received February 20, 2013; Accepted August 27, 2013.
DOI 10.1002/jmri.24435
View this article online at wileyonlinelibrary.com.

can be reduced by increasing the duration of the RF pulse; however, in practice, hardware, T_2 effects with long inversion pulses, and specific absorption rate (SAR) limits, restrict the flexibility to satisfactorily tailor the adiabatic pulse to result in good inversion efficiency over the whole brain. Alternative adiabatic pulses, such as a flattened hyperbolic secant (HS8) (9) or a numerically optimized time resampled frequency offset compensated inversion (TR-FOCI) (10) pulse, have shown to be more suited to cause inversion at a lower B_1^+ than the conventional HS1 pulses (11,12). Yet, any of these pulses will only be effective if there is adequate B_1^+ available.

The elliptical eccentricity of the head is known to influence the spatial inhomogeneity of the transmit field. At 3T, dielectric pads are available to improve the uniformity of the RF distribution in clinical liver imaging (13). For the brain, Yang et al (14) showed that placing water ($\varepsilon_r \approx 80$) bags around the head can improve the homogeneity of the transmit field by reducing its elliptical eccentricity. The practical feasibility of these bags depends on their geometry, specifically the pad's thickness. More recently, Teeuwisse et al (15,16) have shown that the thickness of the pad can be reduced by increasing its permittivity through the use of calcium or barium titanate (15). The simulations of Teeuwisse et al (15) and Yang et al (15,17) both show that with dielectric pads of high relative permittivity between 120 and 180 placed under the neck cause the B_1^+ field's amplitude to increase toward the back of the head. In turbo spin echo (15,17) and MP2RAGE (18) sequences at 7T, it has been shown that very thin (~5 mm) high permittivity ($\varepsilon_r \approx 165$) pads can improve the image quality in the temporal lobes and cerebellum without increasing the inter-coil coupling, the magnetic susceptibility artifacts or the SAR (16,17).

The purpose of this work was to investigate the ability of three different adiabatic pulses, HS1, HS8, and TR-FOCI pulses, in combination with very thin dielectric pads to consistently improve the inversion efficiency for whole-brain MP2RAGE acquisitions, including the cerebellum, over a range of subjects with different head sizes.

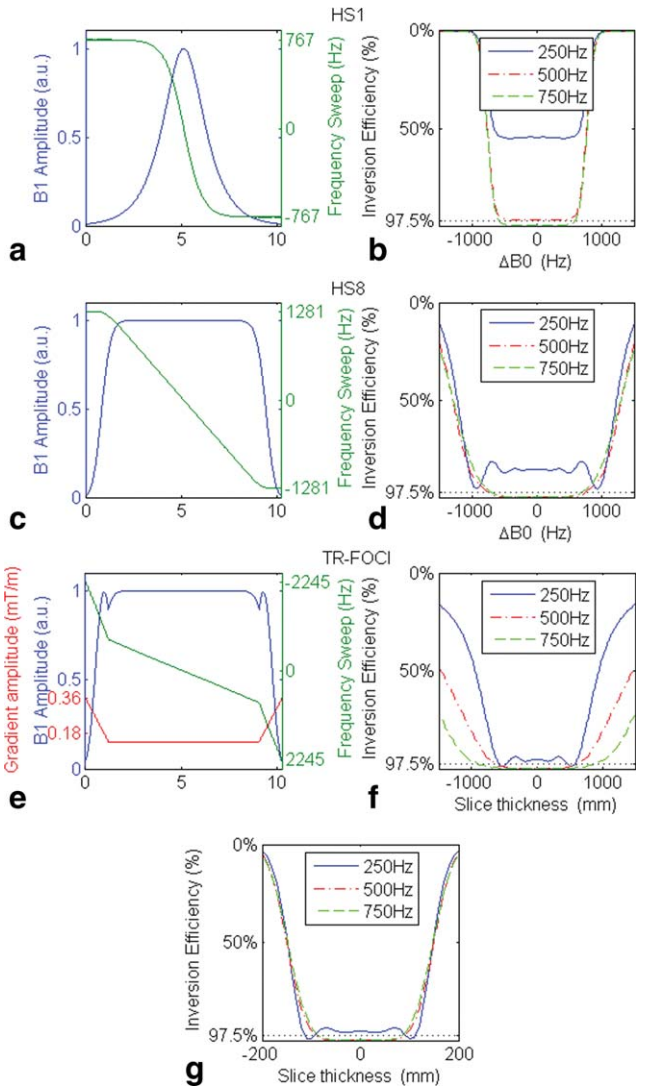

Figure 1. Amplitude, frequency, and gradient modulation (a–c) of the three adiabatic inversion pulses, HS1 (**a,d**), HS8 (**b,e**) and TR-FOCI (**c,f**), as a function of pulse duration along with their corresponding simulated inversion profile as a function of frequency offset (d–f) and slice thickness (**g**) for three different γB_1. The Bloch simulations ignore relaxation.

MATERIALS AND METHODS

Three different adiabatic pulse designs were evaluated for use in whole-brain imaging sequences, such as MP2RAGE. The ΔB_0 offsets across the whole brain were assumed to range between ±500 Hz at 7T (19). The largest offsets occur in the para-nasal sinus, where adequate B_1^+ ($\gamma B_1^+ \geq 500$ Hz) coverage can be expected; therefore, the bandwidths of the HS1 and HS8 pulses were chosen to ensure that a simulated inversion efficiency ≥97.5% is achieved over a ΔB_0 range of ±500 Hz, see Figure 1. For the TR-FOCI pulse, a genetic algorithm as outlined in reference (10) was used to design a 200 mm slab-selective inversion using the HS8 as the base pulse. Edge sharpness is irrelevant for whole-brain slabs, ie, when using a transmit-receive local head coil with restricted transmit field in magnet z-direction; thus, the sharp transition band of an ideal slice profile was replaced with a 50-mm linear ramp to favor pulses with a lower B_1^+ requirement (10). The duration of all three adiabatic pulses were fixed to 10 ms. The operational amplitude for each adiabatic pulse was chosen to either comply with the peak amplitude available on the system (HS1), or the maximum B_1^+ amplitude that allowed the scan to be performed within the SAR limits (HS8/TR-FOCI).

Two sets of dielectric pads were constructed as specified in reference (15). Three MR visible pads, measuring 110 × 110 mm^2, were filled with a slurry mix of distilled water and barium titanate (total volume 30 mL, volume-to-fluid ratio of 25%). To avoid fluid displacement (15,16) from the back of the neck, a second set of three smaller MR-invisible dielectric pads measuring 70 × 70 mm^2, filled with a mix of deuterated water and barium titianate (total volume

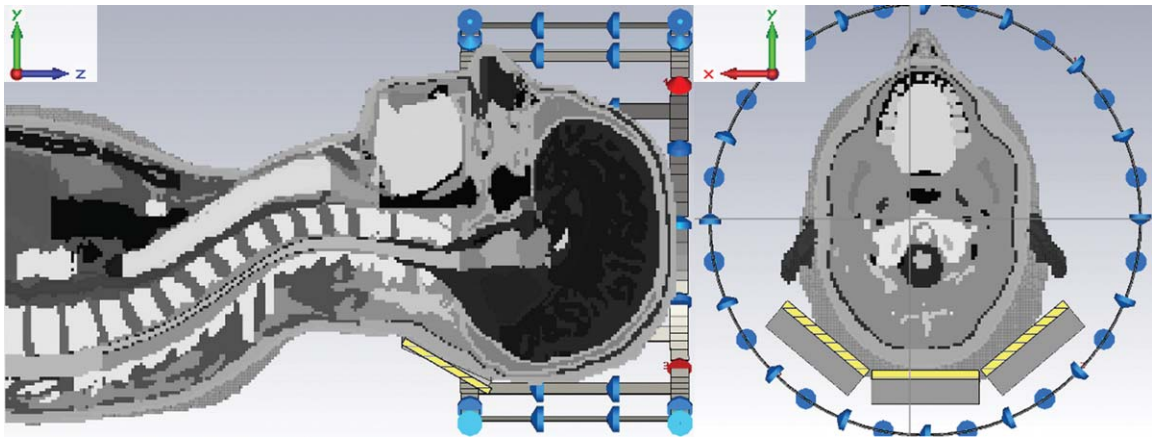

Figure 2. The position of the dielectric pads in the simulations was chosen to best match their placement in the scanner. They were placed underneath the back of the head/neck, just below the ears.

30 mL, volume to fluid ratio of 25%), were also constructed. To verify that an increase in the available B_1^+ occurs over the cerebellum and no change in peak 10g SAR occurs, the RF field distribution and corresponding SAR maps produced by the RF coil were simulated using Microwave Studio (CST, Darmstadt, Germany). The coil was loaded with an anatomically detailed human head model (Duke from the Virtual Family) (20). Simulations were run with and without the three dielectric pads present. The coil was modeled as a 16-rung birdcage with approximately the same dimensions as the transmit coil used in our experimental setup. Dielectric pads were modeled as blocks ($70 \times 70 \times 5$ mm^3, $\varepsilon_r = 165$, $\tan\delta = 0.04$) (15) positioned on the back of the head at the top of the neck and behind the ears (Fig. 2). The B_1^+ field from the simulation without dielectric pads was scaled to reach $\gamma B_1^+ = 500$ Hz at the center of the head. The B_1^+ field from the simulation with dielectric pads was then scaled by the same factor. SAR maps from both simulations are presented relative to 1 W accepted power at the coil.

Three different in vivo experiments were performed. In experiment 1, the inversion efficiencies of the HS1/HS8/TR-FOCI adiabatic pulses were assessed on whole-brain MP2RAGE acquisitions from four subjects ($TR_{MP2RAGE}$/ $TR_{READOUT}$/TE 5.5 s/6.6 ms/2.84 ms α_1/α_2 $4^\circ/5^\circ$ TI_1/TI_2 0.75 s/2.35 s Matrix $320 \times 280 \times 208$, voxel $1.0 \times 1.0 \times 1.2$ mm). Second, in experiment 2, the four subjects (29.7 ± 1.7 years; 3 male), underwent a repeat scan session with the three MR-visible dielectric pads: one placed under the neck and two placed on either side just below the ears. Finally, to assess the performance reliability of the dielectric pads, experiment 3 acquired MP2RAGE using the TR-FOCI adiabatic pulse and the MR-invisible dielectric pads from eight subjects (29.0 ± 4.1 years; 6 Male) in two separate scan sessions ($TR_{MP2RAGE}/TR_{READOUT}$/TE 6 s/6.5 ms/2.89 ms α_1/α_2 $4^\circ/5^\circ$ TI_1/TI_2 0.8 s/2.7 s Matrix $256 \times 240 \times 176$, voxel $1.0 \times 1.0 \times 1.2$ mm). Note, the $TR_{MP2RAGE}$ was increased to further reduce the SAR deposition and to allow the application/use of a higher peak amplitude of the TR-FOCI pulse. All scans were approved by the local institutional ethics committee and informed consent was obtained for all subjects.

All scans were performed on a Magnetom 7 T /680 mm human scanner (Siemens Healthcare Sector, Erlangen, Germany) with a head-gradient insert (max 80 mT/m and 333 T/m/s) using a single-channel quadrature transmit RF coil (physical length ~180 mm) and a 32-channel receive array coil (NM068-32-7S, Nova Medical Inc, MA). Subjects were carefully positioned, so that the top of their heads were as close as possible to the internal edge of the receive coil. The reference voltage of the transmitter was fixed to 250 V for all subjects. After initial shimming and frequency adjustment with the manufacturer's standard procedure, a customized whole head three-dimensional (3D) GRE (TR/TE_1 8.1 ms/2.04 ms, Matrix $96 \times 96 \times 64$, voxel $3.1 \times 3.1 \times 3.1$ mm) shimming/frequency adjustment procedure (21) was applied by increasing the ΔTE from 2.04 ms in the first volume to a ΔTE of 4.08 ms in the second volume. B_1^+ maps were obtained with a SA2RAGE (22) acquisition (TR/TE 2400/0.72 ms, matrix $116 \times 128 \times 64$, voxel $2.3 \times 2.3 \times 4$ mm). The preparation procedure was performed for each subject and took a total time of 4 min. To compare the effect of the dielectric pads on the ΔB_0 distribution over the brain a third 3D GRE volume with ΔTE4.08 ms was also acquired.

To compare the effect of the dielectric pads on the B_1^+ maps they were initially co-registered using customized Matlab (Mathworks, Natick, MA) scripts. The B_1^+ amplitude for each adiabatic pulse (B_1^{Inv}) can be calculated by

$$B_1^{Inv} = B_1^{Ref} \frac{V^{op}}{V^{ref}} \quad [1]$$

using the fixed reference voltage (V^{ref}), the operational amplitude of each pulse (V^{op}), and the reference amplitude of the pulse used to create the B_1^+ maps (B_1^{Ref}). The ΔB_0 maps were determined offline, and phase wraps were removed using a iterative weighted least squares solution to Poisson's equation using fast cosine transforms (23).

The inversion efficiency of the adiabatic pulses was qualitatively assessed on the uniform MP2RAGE

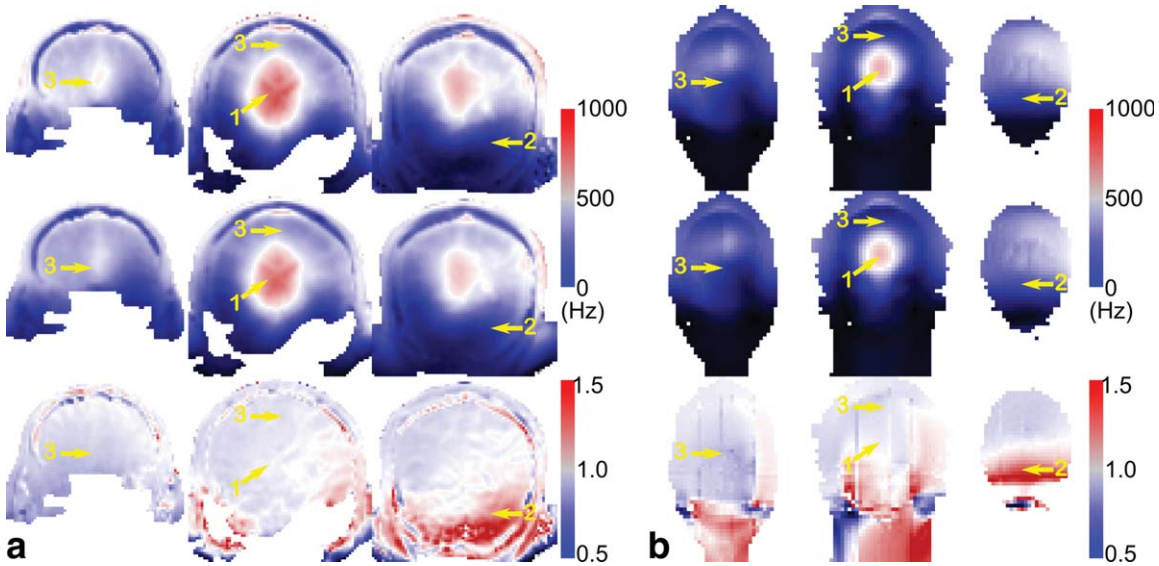

Figure 3. Measured (**a**), using subject 3, and simulated (**b**) B_1^+ maps without (top row) and with (middle) dielectric cushions, and their ratio (bottom) for three coronal slice positions show that the central region of high B_1^+ (1) moves to favor B_1^+ distribution over the cerebellum (2) at the expense of anterior and superior regions (3). The change in the simulated RF field's distribution shows good agreement with the measured data.

image, which were calculated using the complex ratio described in (1). In this image, poor inversion results in artificially bright signal intensities in the uniform image of the MP2RAGE acquisition. To assess the impact of the dielectric pads on the inversion efficiency, all the MP2RAGE image volumes were co-registered to the TR-FOCI MP2RAGE image volume (2nd gradient echo contrast $TI_2 = 2.7$ s) acquired with dielectric pads. The presence, or lack, of a poor inversion artifact was qualitatively compared with the head dimensions and position of the brain inside the coil. The measurements were taken from the 3D MP2RAGE images, except for the circumference which was measured externally with a tape measure.

To quantify the B_1^+ available to cause inversion, the B_1^+ maps were co-registered to the TR-FOCI MP2RAGE images and regions of interest were manually placed over the frontal, anterior, central, temporal lobe and cerebellum. Care was taken to ensure that if present the regions of interest contained the areas of poor inversion.

The MP2RAGE images from the repeat scans were similarly co-registered to each other using the 2nd gradient echo contrast. Whilst viewing the uniform images simultaneously, the images were qualitatively assessed for the presence, or lack, of a poor inversion artifact (bright signal intensities) by two observers (K.O./G.K.) who are familiar with the artifact on MP2RAGE images. In each image shown herein, the slice with the worst residual inversion artifact is presented.

RESULTS

The amplitude envelope, frequency sweep and gradient profiles (if appropriate) of the HS1 (a), HS8 (b), and TR-FOCI (c) adiabatic pulses, and the simulated frequency (d–f) or slice (g) profiles are given in Figure 1. The simulated profiles show that at a $\gamma B_1^+ = 500$ Hz, the desired inversion efficiency can be achieved by each pulse. The TR-FOCI pulse reaches the desired inversion efficiency at the lowest γB_1^+ (~280 Hz), and the HS8 was lower (~340 Hz) than the HS1 pulse (500 Hz). However, the operational amplitude that could be achieved by the HS1 pulse was higher (≈520 V, the

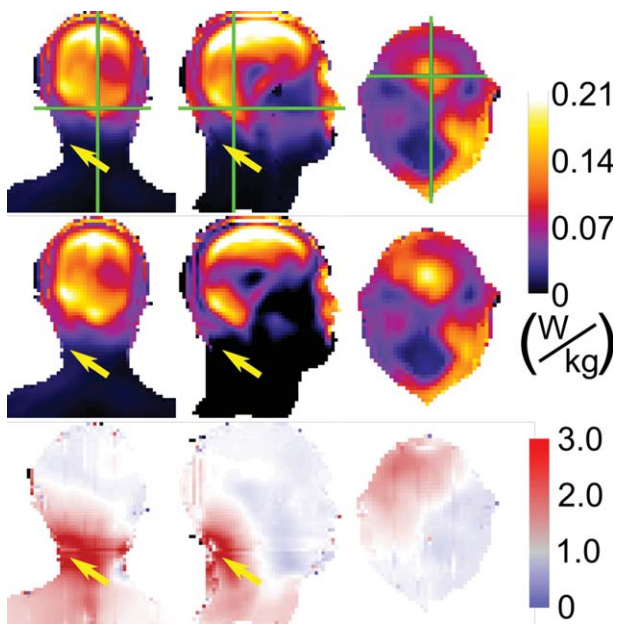

Figure 4. Coronal, sagittal, and transverse slices (green crosshairs) of the simulated local 10g-averaged SAR maps, relative to a peak accepted power of 1 W at the coil, without (top row) and with (middle) dielectric pads; and their ratio (bottom). The region of largest increase (arrow) in local 10g-average SAR occurs in a region of low SAR deposition.

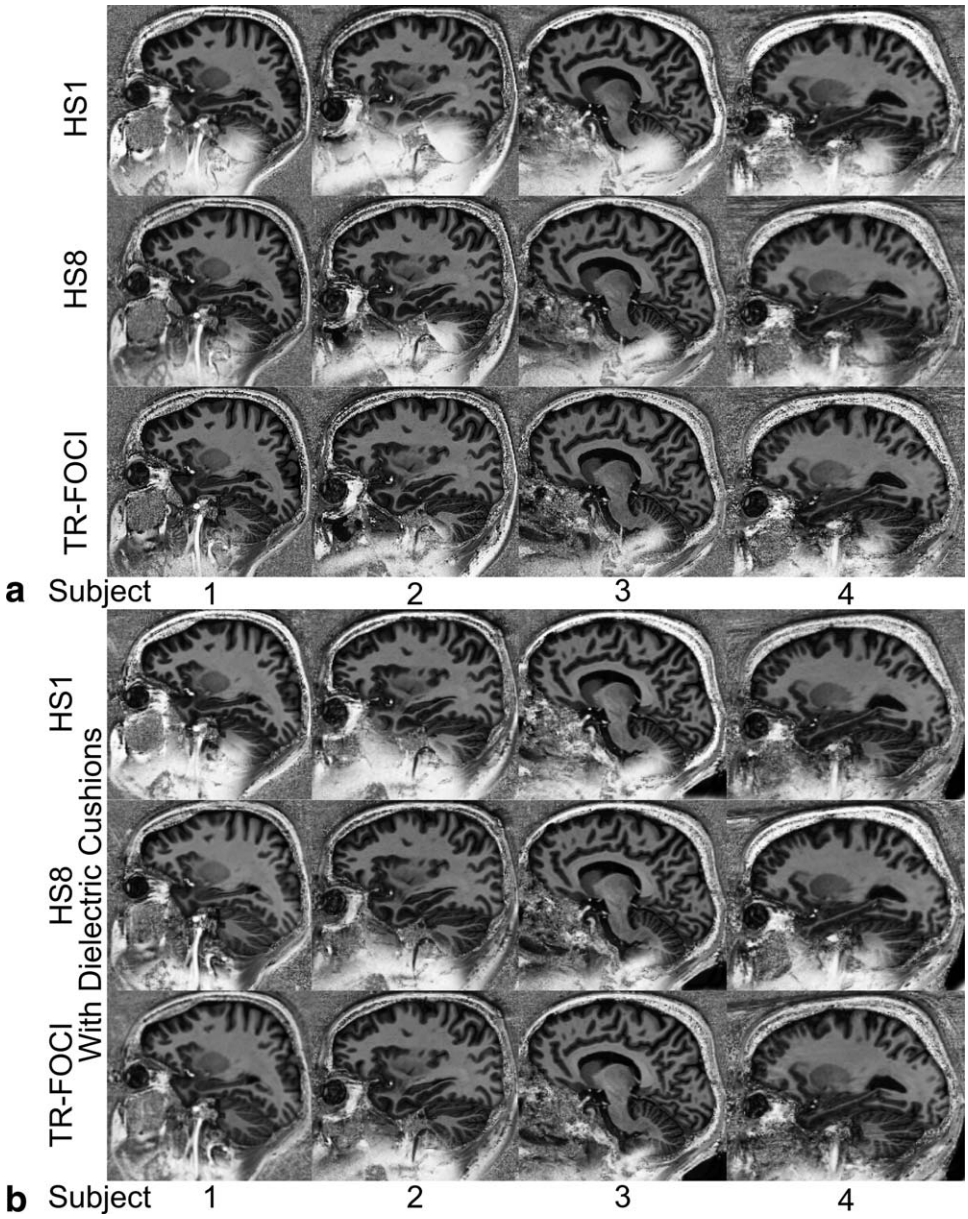

Figure 5. a,b: Sagittal cross-section for each of the four subjects showing the effect of using different adiabatic inversion pulses and the dielectric cushions. Poor inversion is characterized by a bright signal intensity. A dielectric pad, whose signal intensity is similar to cerebrospinal fluid, is visible in the lower right corner.

maximum available with the system/coil combination). In comparison the HS8 and TR-FOCI pulses distribute the RF energy over the entire duration of the pulse, which means that their operational amplitude was restricted due to SAR constraints. Thus, for the protocol parameters used in experiments 1 and 2, the operational amplitudes of the HS8 and TR-FOCI pulses were ≈430 V and ≈410 V, respectively. Given the fixed reference voltage of 250 V and the simulated minimum B_1^+ amplitude for each adiabatic pulse (B_1^{Inv}), the required B_1^{Ref} to achieve inversion can be calculated for each pulse from Eq. (1): HS1 $\gamma B_1^+ = 240$ Hz, HS8 $\gamma B_1^+ = 200$ Hz and TR-FOCI $\gamma B_1^+ = 170$ Hz.

The simulations of the RF field distribution with and without the MR-invisible dielectric pads correspond with what is measured in vivo (Fig. 3). The corresponding SAR maps (Fig. 4) show that, while the local 10g-averaged SAR is increased in regions close to the pads, the location of the peak local 10g-averaged SAR remains unchanged at the top of the head. In fact, the peak local 10g-averaged SAR reduces by 6% from 0.345 W/kg to 0.324 W/kg with the dielectric pads placed as shown in Figure 2. In contrast, the average SAR over the whole head remains relatively unchanged at 0.0244 W/kg and 0.0245 W/kg.

The effect of using the low-B_1^+ adiabatic pulses is shown in Figures 5 and 6. The HS1 pulse does not provide an adequate inversion in the cerebellum in all subjects. Replacing the inversion pulse with either a HS8 or TR-FOCI pulse displaces the poor inversion artifact toward the neck and achieves improved inversion over the cerebellum.

The head dimensions and the required z-coverage of the B_1^+ field (measured from the superior edge of the head to the inferior edge of the cerebellum) along with B_1^+ measurements from regions of interest in the brain are given in Table 1. In subjects 1–3, residual poor inversion artifacts were present along the inferior edge of the cerebellum close to the brain stem. The

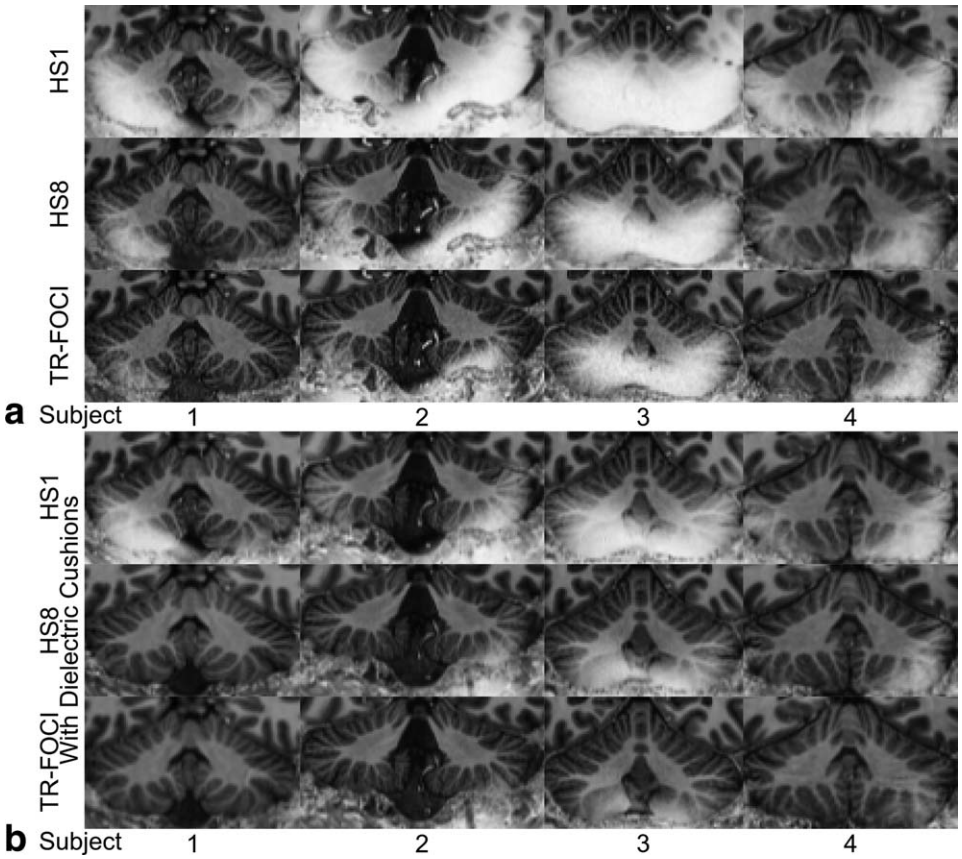

Figure 6. a,b: Coronal zoomed cross-section of the cerebellum for each subject showing the effect of using different adiabatic inversion pulses without (row 1–3) and with the dielectric pads (row 4–6). Poor inversion is characterized by bright signal intensity.

extent of the artifact was more pronounced in subjects who required a larger z-coverage of the B_1^+ field. Additionally, subject 4, who had the most eccentric head shape, has a residual artifact in the temporal lobes (data not shown). Consequently, the addition of dielectric pads further improves the inversion efficiency of all pulses over the cerebellum and temporal lobes as shown in Figures 5 and 6. When combined with the pads, the HS8 and TR-FOCI pulses still outperform the HS1 pulse; however, small residual artifacts occasionally persist along the inferior cerebellum close to the brain stem.

Table 1
Head Dimensions and B_1^+ Measurements From Regions of Interest in the Brain for 4 Subjects

Subject		1	2	3	4
Head dimensions (mm)	Sup. – Inf.	190	200	210	230
	Ant. – Post.	174	195	201	206
	Left – Right	155	152	169	149
	Circumference	550	590	610	600
	Meridonal Ecc.	0.50	0.50	0.47	0.64
	Equatorial Ecc.	0.45	0.63	0.54	0.69
	Sup. – Inf. cer	149	150	163	151
γB_1^+ values without pads (Hz)	Frontal	473 ± 67	404 ± 26	389 ± 23	490 ± 21
	Anterior	517 ± 70	364 ± 16	422 ± 20	413 ± 14
	Central	727 ± 101	587 ± 43	632 ± 31	628 ± 34
	Temporal	240 ± 106	208 ± 47	235 ± 46	193 ± 60
	Cerebellum	231 ± 37	194 ± 49	125 ± 37	198 ± 19
γB_1^+ values with pads (Hz)	Frontal	403 ± 26	410 ± 25	388 ± 30	449 ± 14
	Anterior	416 ± 56	369 ± 15	402 ± 18	368 ± 11
	Central	642 ± 55	589 ± 43	609 ± 36	588 ± 32
	Temporal	316 ± 43	212 ± 46	274 ± 57	209 ± 74
	Cerebellum	299 ± 88	254 ± 60	187 ± 52	292 ± 17
% change of B_1^+ (with/without)	Frontal	−15% ± 16%	1% ± 9%	-13% ± 11%	−8% ± 5%
	Anterior	−20% ± 19%	1% ± 6%	−5% ± 6%	−11% ± 4%
	Central	−12% ± 16%	0% ± 10%	−4% ± 8%	−6% ± 8%
	Temporal	32% ± 46%	2% ± 32%	16% ± 28%	8% ± 47%
	Cerebellum	29% ± 34%	31% ± 35%	50% ± 40%	48% ± 11%

Sup = superior; Inf = inferior; Ant = anterior; Post = posterior; Ecc = eccentricity; cer = cerebella edge.

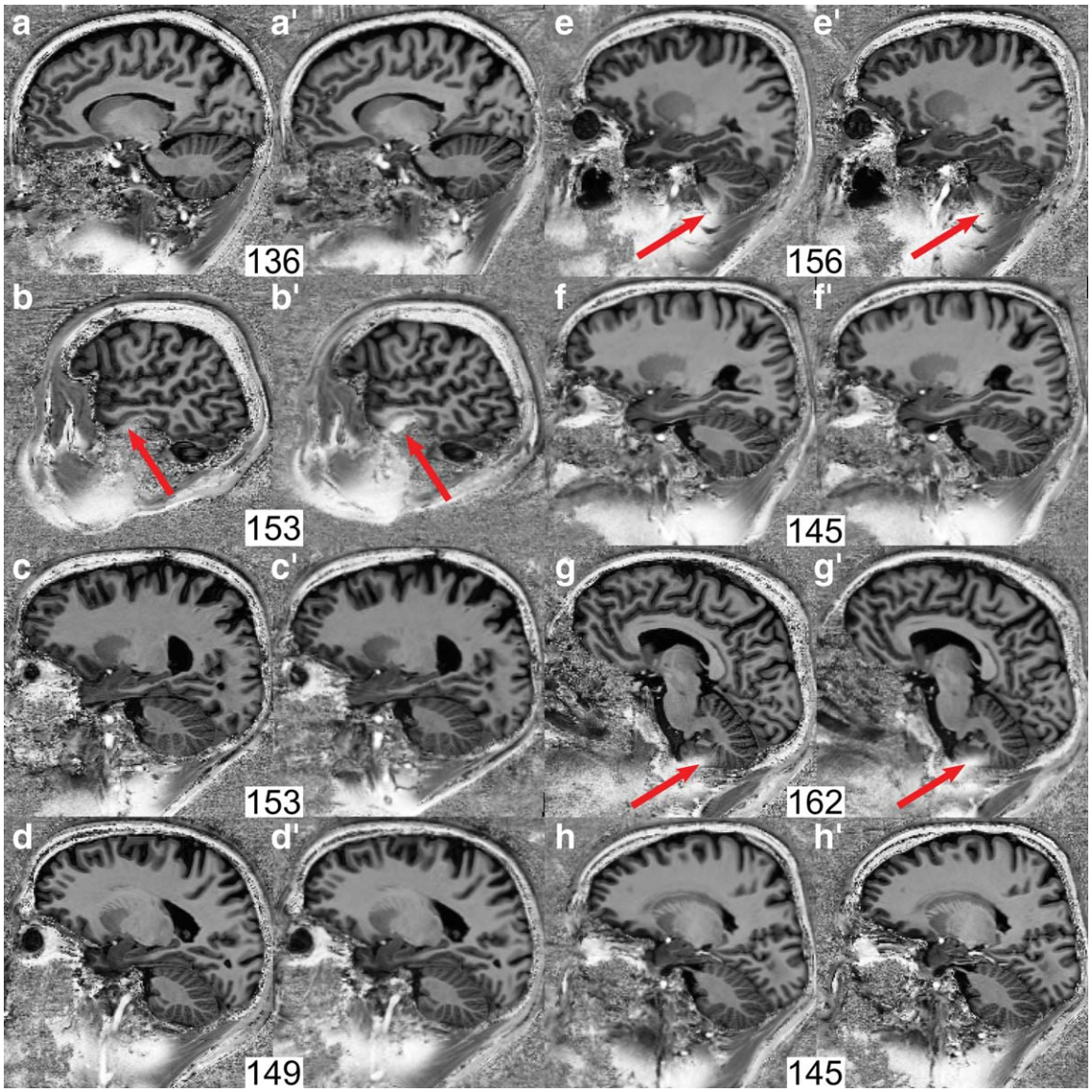

Figure 7. Sagittal slices, chosen to show residual inversion artifacts if present (black arrows), from each of the eight subjects (**a–h**) and their repeat scans (a′–h′) showing good inversion over the entire brain. The required z-coverage is given (in mm) for each subject.

The effect of the dielectric pads, when positioned at the bottom of the cerebellum, is to displace the region of high RF amplitude at the brain center toward the cerebellum (Fig. 3). The available B_1^+ increases by up to 50% over the cerebellum, while the improvement in the temporal lobes was more modest. The improvement comes at the expense of B_1^+ in the anterior and superior regions of the head; however, as these regions have a higher initial B_1^+, complete inversion is still achieved. The mean($\pm\sigma$) ΔB_0 distribution over the brain with (-4.2 ± 95.2 Hz) and without (4.2 ± 103.6 Hz) the pads remains unchanged, suggesting that the observed changes in the inversion efficiency arise only from the modulation of the B_1^+ field by the pads.

To test the reliability of using the dielectric pads to improve the inversion efficiency in the cerebellum and temporal lobes, we compared the MP2RAGE scans of eight subjects from two different scan sessions. The longer $TR_{MP2RAGE}$ allowed the operation amplitude of the TR-FOCI pulse to be increased by ≈5% to ≈430 V. Whole-brain coverage was consistently achieved in most subjects in both sessions, see Figure 7. Complete coverage of the cerebellum was achieved in all subjects who had a required z-coverage of the B_1^+ field <155 mm. Small residual poor inversion artifacts at the inferior edge of the cerebellum were present in two of eight subjects, and in one subject poor inversion was present in the temporal lobe for one repetition.

DISCUSSION

In this work, we found that the use of dielectric pads and low-B_1^+ adiabatic pulses are two complementary techniques that improve the inversion efficiency across the whole brain for MP2RAGE acquisitions. Specifically, the use of adiabatic pulses such as the HS8 and TR-FOCI, which allow inversion to occur at a

lower B_1^+ than the conventional HS1 pulse and the use of dielectric pads to change the B_1^+ distribution over the brain.

With the current hardware and SAR constraints, either an HS8 or TR-FOCI pulse improves the inversion coverage over the whole brain compared with the conventional HS1 pulse. The lower adiabatic threshold of the TR-FOCI pulse compensates for the larger SAR requirement, which restricts its operational amplitude compared with the HS8 pulses. Increasing the TR further, eases the SAR restrictions on the maximum amplitude of the HS8 and TR-FOCI adiabatic pulses and further improves the inversion coverage. In particular in subjects (eg, subject 3) where the available B_1^+ is low, ie, $\leq$135 Hz, then the minimum operational voltage required for complete inversion coverage is estimated to be in excess of $\geq$630 V and $\geq$520 V for the HS8 and TR-FOCI pulses, respectively. However, due to SAR, this may result in unsatisfactorily long acquisition times.

Rather than the eccentricity of a subject's head, the residual limitations in inversion efficiency were largely driven by the rapid drop off of the transmit field's z-coverage. In those subjects where the required z-coverage of the B_1^+ field needed to incorporate the cerebellum was large the B_1^+ available became insufficient to exceed the adiabatic threshold. Dielectric pads offer an effective and simple solution to increase the B_1^+ amplitudes in these areas.

For whole head coverage, the B_1^+ can be increased by up to 50% over the cerebellum with generally only small losses ($\leq$20%) in the anterior and superior regions of the head. Apart from ensuring adequate B_1^+ is available for inversion in the cerebellum, the effect of the pads will also result in actual flip angles that are now closer to the anticipated flip angle. In the frontal and superior regions, there will be a small loss in the actual flip angles compared with the anticipated flip angle. Overall, the greater improvement of the B_1^+ field over the cerebellum outweighs the small loss in the frontal and superior regions creating a more homogeneous excitation over the brain (mean $\pm$ σ across subjects was $\gamma B_1^+ = 428 \pm 139$ Hz without compared with $\gamma B_1^+ = 408 \pm 104$ Hz with dielectric pads). Thus, the realized signal and contrast to noise ratios of the MP2RAGE uniform image will be better matched to the desired signal and contrast to noise ratios (2).

The reference voltage required to achieve the same flip angle at the center of the brain is slightly larger with the dielectric pads present; therefore, it could be argued that the pads may cause a slight increase in the global SAR (16) but, if averaged over the whole brain, the reference voltage remains similar. This allows the application of the same fixed reference voltage for all subjects, which causes the global SAR to be unaffected by the dielectric pads. Moreover, the simulations showed that local 10g-averaged SAR restrictions will still dominate the safety calculations at 7T. Positioning the pads underneath the back of the head/neck does cause the local 10g-averaged SAR in adjacent tissue to increase; however, this region has a low SAR deposition both before and after positioning the dielectric pads. The position of the peak local 10g-averaged SAR remains unchanged and in fact is slightly lower than with no pads present. Thus, the presence of the pads under the head/neck does not affect standard operating procedures.

In other specific imaging scenarios, eg, targeted imaging of the cerebellum, where one would also position the pads under the head/neck as proposed throughout the paper, a lower reference voltage can be expected; hence, a lower SAR will be achieved with the use of the dielectric pads. However, positioning the pads more anterior, or on top of the head, may result in a change in the local SAR distribution that does increase the peak local SAR. Hence, before using dielectric pads in locations other than the back of the neck, it is essential to ensure that the peak local SAR is not increased.

Subject-specific RF pulses that can be tailored to improve inversion in regions of low- B_1^+ have been proposed (24,25) to improve inversion efficiency over the whole brain. However, these pulses are better suited to parallel transmission applications, where the multiple transmit coils can be used to improve the homogeneity of the transmit field. The use of dielectric pads does not affect standard operating procedures; yet, it can reproducibly improve the inversion efficiency in the cerebellum and temporal lobes for all subjects.

The inversion artifacts still present on the inferior edge of the cerebellum limits whole-brain T_1w acquisitions to subjects whose required z-coverage is $\leq$155 mm. Full coverage is limited by the operational amplitude of the low-B_1^+ adiabatic pulse and the z-coverage of the coil. Therefore with the current SAR constraints, further improvements could be best obtained if the B_1^+ field of the coil was designed to better cover the cerebellum. Increasing the relative permittivity of the dielectric pads or increasing their thickness may also increase the B_1^+ over the cerebellum further but at the expense of greater losses in the anterior and frontal regions. Lastly, as reported by Teeuwisse et al (15,16), the reliability of the dielectric pads placement could be further improved if a series of smaller pads were inserted into a head cushion that could be molded to the subject's head.

In conclusion, the use of dielectric pads, placed under the head/neck, in conjunction with a low-B_1^+ adiabatic pulse improves the inversion efficiency in the cerebellum to a level that allows robust whole-brain images with more homogeneous signal and T_1w contrast at 7T. Residual artifacts that can be observed in some subjects are largely driven by large head size and the reduced spatial coverage of the B_1^+ field. Therefore, for subject's whose required z-coverage is $\leq$155 mm, the dielectric pads in-conjunction with the TR-FOCI pulse enable whole-brain structural T_1w scans free of inversion artifacts.

ACKNOWLEDGMENTS

This work was supported by the Leenaards and Jeantet Foundations and the Centre d'Imagerie Biomédicale (CIBM) from the UNIL, UNIGE, HUG, CHUV, EPFL.

REFERENCES

1. Marques JP, Kober T, Krueger G, van der Zwaag W, Van de Moortele P-F, Gruetter R. MP2RAGE, a self bias-field corrected sequence for improved segmentation and T1-mapping at high field. Neuroimage 2010;49:1271–1281.
2. Van de Moortele P-F, Auerbach EJ, Olman C, Yacoub E, Ugurbil K, Moeller S. T1 weighted brain images at 7 Tesla unbiased for Proton Density, T2* contrast and RF coil receive B1 sensitivity with simultaneous vessel visualization. Neuroimage 2009;46:432–446.
3. Marques JP, Gruetter R. New developments and applications of the MP2RAGE sequence - focusing the contrast and high spatial resolution R1 Mapping. PLoS One 2013;8:e69294.
4. Whitwell J, Crum W, Watt W, Fox N. Normalization of cerebral volumes by use of intracranial volume: implications for longitudinal quantitative MR imaging. AJNR Am J Neuroradiol 2001;22: 1483–1489.
5. Van de Moortele P-F, Akgun C, Adriany G, et al. B1 destructive interferences and spatial phase patterns at 7 T with a head transceiver array coil. Magn Reson Med 2005;54:1503–1518.
6. Vaughan JT, Garwood M, Collins CM, et al. 7T vs. 4T: RF power, homogeneity, and signal-to-noise comparison in head images. Magn Reson Med 2001;46:24–30.
7. Adriany G, Van de Moortele P-F, Wiesinger F, et al. Transmit and receive transmission line arrays for 7 Tesla parallel imaging. Magn Reson Med 2005;53:434–445.
8. Tannús A, Garwood M. Adiabatic pulses. NMR Biomed 1997;10: 423–434.
9. Garwood M, DelaBarre L. The return of the frequency sweep: designing adiabatic pulses for contemporary NMR. J Magn Reson 2001;153:155–177.
10. Hurley AC, Al-Radaideh A, Bai L, et al. Tailored RF pulse for magnetization inversion at ultrahigh field. Magn Reson Med 2009;63: 51–58.
11. Wrede KH, Johst S, Dammann P, et al. Caudal image contrast inversion in MPRAGE at 7 Tesla: problem and solution. Acad Radiol 2012;19:172–178.
12. O'Brien K, Delacoste J, Marques J, Krueger G.Improving the inversion efficiency in regions of low γB1 for whole brain acquisitions. In: Proceedings of the 20th Annual Meeting of ISMRM, Melbourne, Australia, 2012.
13. Schmitt M, Feiweier T, Horger W, et al.Improved uniformitty of RF-distribution in clinical whole body-imaging at 3T by means of dielectic pads. In: Proceedings of the 12th Annual Meeting of ISMRM, Kyoto, Japan; 2004. p. 954.
14. Yang QX, Wang J, Wang J, Collins CM, Wang C, Smith MB. Reducing SAR and enhancing cerebral signal-to-noise ratio with high permittivity padding at 3 T. Magn Reson Med 2011;65:358–362.
15. Teeuwisse WM, Brink WM, Haines KN, Webb AG. Simulations of high permittivity materials for 7 T neuroimaging and evaluation of a new barium titanate-based dielectric. Magn Reson Med 2012;67:912–918.
16. Teeuwisse WM, Brink WM, Webb AG. Quantitative assessment of the effects of high-permittivity pads in 7 Tesla MRI of the brain. Magn Reson Med 2012;67:1285–1293.
17. Yang QX, Rupprecht S, Luo W, et al. Radiofrequency field enhancement with high dielectric constant (HDC) pads in a receive array coil at 3.0T. J Magn Reson Imaging 2013;38:435–440.
18. O'Brien K, Kober T, Marques J, Lazeyras F, Gruetter R, Krueger G.High quality whole brain MP2RAGE at 7T: utilization of thin dielectric pads. In: Proceedings of the 21st Annual Meeting of ISMRM, Salt Lake City, Utah, 2013. p. 3009.
19. Juchem C, Nixon TW, Diduch P, Rothman DL, Starewicz P, de Graaf RA. Dynamic shimming of the human brain at 7 Tesla. Concepts Magn Reson Part B Magn Reson Eng 2010;37B:116–128.
20. Christ A, Kainz W, Hahn EG, et al. The virtual family—development of surface-based anatomical models of two adults and two children for dosimetric simulations. Phys Med Biol 2010;55:N23–N38.
21. Greiser A, Weber O, Deshpande V, Mueller E. Improved cardiac shimming in a clinical setting by multi-frame fieldmap acquisition and automatic ROI extension. J Cardiovasc Magn Reson 2007;9: 239.
22. Eggenschwiler F, Kober T, Magill AW, Gruetter R, Marques JP. SA2RAGE: a new sequence for fast $B1^{+}$-mapping. Magn Reson Med 2012;67:1609–1619.
23. Ghiglia DC, Romero LA. Robust two Dimensional weighted and unweighted phase unwrapping that uses fast transforms and iterative methods. J Opt Soc Am A 1994;11.
24. Cloos M, Boulant N, Luong M, et al.kT-points-based inversion pulse design for transmit-SENSE enabled MP-RAGE brain imaging at 7T. In: Proceedings of the 20th Annual Meeting of ISMRM, Melbourne, Australia, 2012 (abstract 634).
25. Cloos MA, Boulant N, Luong M, et al. kT-points: short three-dimensional tailored RF pulses for flip-angle homogenization over an extended volume. Magn Reson Med 2012;67:72–80.